The Canadian Mineralogist
Vol. 41, pp. 1433-1444 (2003)

SCHLEMAITE, $(Cu,\square)_6(Pb,Bi)Se_4$, A NEW MINERAL SPECIES FROM NIEDERSCHLEMA–ALBERODA, ERZGEBIRGE, GERMANY: DESCRIPTION AND CRYSTAL STRUCTURE

HANS-JÜRGEN FÖRSTER[§]

Institute of Earth Sciences, University of Potsdam, D–14415 Potsdam, Germany

MARK A. COOPER

Department of Geological Sciences, University of Manitoba, Manitoba R3T 2N2, Canada

ANDREW C. ROBERTS

Geological Survey of Canada, 601 Booth Street, Ottawa, Ontario K1A 0E8, Canada

CHRIS J. STANLEY AND ALAN J. CRIDDLE[†]

Department of Mineralogy, Natural History Museum, Cromwell Road, London SW7 5BD, U.K.

FRANK C. HAWTHORNE

Department of Geological Sciences, University of Manitoba, Manitoba R3T 2N2, Canada

J.H. GILLES LAFLAMME

CANMET, 555 Booth Street, Ottawa, Ontario K1A 0G1, Canada

GERHARD TISCHENDORF

Bautzner Strasse 16, D–02763 Zittau, Germany

ABSTRACT

Schlemaite, with the simplified formula $(Cu,\square)_6(Pb,Bi)Se_4$, is a new mineral species from the Niederschlema–Alberoda vein-type uranium deposit at Hartenstein, Erzgebirge, Germany. It occurs as anhedral to subhedral grains with no obvious forms or twinning, in aggregates of up to several hundred μm across, with berzelianite, eucairite and clausthalite in a dolomite–ankerite matrix. Schlemaite is black with a black streak and opaque with a metallic luster. It is brittle with an uneven fracture and no observable cleavage. It has a mean VHN (25 g load) of 106 kg/mm^2, which roughly equates to a Mohs hardness of 3. In plane-polarized reflected light, schlemaite is grey, non-pleochroic with a very weak bireflectance. It has very weak anisotropy, with rotation tints in shades of very pale metallic orange and blue, and shows no internal reflections. Electron-microprobe analyses yielded a mean composition Cu 38.86, Ag 2.57, Au 0.07, Hg 0.09, Pb 13.75, Bi 9.12, Se 35.11, total 99.57 wt.%. The empirical formula (based on 4 Se *apfu*) is $(Cu_{5.50}Ag_{0.21})_{\Sigma 5.71}(Pb_{0.60}Bi_{0.39})_{\Sigma 0.99}Se_4$. The calculated density is 7.54 g/cm^3 (based on the empirical formula and unit-cell parameters refined from single-crystal data). Schlemaite is monoclinic, $P2_1/m$, a 9.5341(8), b 4.1004(3), c 10.2546(8) Å, β 100.066(2)°, V 394.72(9) Å^3, $a{:}b{:}c$ 2.3252:1:2.5009, $Z = 2$. The crystal structure of schlemaite was solved by direct methods and refined to an R index of 4.8% using 1303 unique reflections collected on a four-circle diffractometer equipped with a CCD detector. The structure consists of intercalated ordered and disordered layers. The ordered layer consists of ladders of $Pb^{2+} + Bi^{3+}$ coordinated by Se, the former showing strong lone-pair-stereoactive effects, and a network of Cu^+ coordinated by Se anions. The disordered layer consists of an array of sites partly occupied by Cu^+ and Ag^+ in a variety of coordinations, and is characterized by strong short-range order. The strongest seven lines of the X-ray powder-diffraction pattern [d in Å(I)(hkl)] are:

[§] *E-mail address*: for@geo.uni-potsdam.de

[†] Deceased, May 2002.

3.189(100)(012), 3.132(100)$(\bar{1}12)$, 2.601(70)$(\bar{1}13)$, 2.505(50)$(\bar{3}11)$, 2.151(60)(014), 2.058(80)(020) and 1.909(50)$(\bar{3}14)$. Although schlemaite is chemically similar to furutobeite, $(Cu,Ag)_6PbS_4$, it is not isostructural with it. The mineral is named after the Schlema–Alberoda uranium ore field near Schneeberg in the ancient mining region of Saxony, Germany.

Keywords: schlemaite, new mineral species, Cu–Pb–Bi selenide, eucairite, berzelianite, electron-microprobe data, reflectance data, crystal structure, X-ray data, Niederschlema–Alberoda, Erzgebirge, Germany.

SOMMAIRE

La schlemaïte, dont la formule simplifiée est $(Cu,\square)_6(Pb,Bi)Se_4$, est une nouvelle espèce minérale découverte dans le gisement d'uranium de type filonien de Niederschlema–Alberoda à Hartenstein, Erzgebirge, en Allemagne. Elle se présente sous forme de grains idiomorphes à sub-idiomorphes, sans formes évidentes, ni macle, et typiquement en aggrégats jusqu'à plusieurs centaines de micromètres de diamètre, avec la berzélianite, la eucairite et la clausthalite dans une matrice à dolomite–ankérite. La schlemaïte est noire, opaque avec un reflet métallique, et possède une rayure noire. Elle est fragile, avec une fracture inégale, et semble sans clivage. Elle a une microdureté VHN_{25} de 106 kg/mm^2, en moyenne, ce qui équivaut à une dureté de Mohs de 3. Observée au microscope polarisant en lumière réfléchie, la schlemaïte est grise, ne présente pas de pléochroïsme et est faiblement biréflectante. L'anisotropie est très faible, et elle montre des teintes de rotation aux nuances qui passent de l'orangé métallique très pâle au bleu, et ne possède pas de réflexions internes. Les analyses obtenues à la microsonde électronique ont donné, en moyenne, Cu 38.86, Ag 2.57, Au 0.07, Hg 0.09, Pb 13.75, Bi 9.12, Se 35.11, total 99.57% en poids. La formule empirique (sur une base de 4 atomes Se par unité de formule, *apuf*) est $(Cu_{5.50}Ag_{0.21})_{\Sigma 5.71}$ $(Pb_{0.60}Bi_{0.39})_{\Sigma 0.99}Se_4$. La densité calculée est égale à 7.54 g/cm^3 (sur la base de la formule empirique et des paramètres de la maille élémentaire déterminés sur un monocristal). La schlemaïte est un minéral monoclinique, avec a 9.5341(8), b 4.1004(3), c 10.2546(8) Å, β 100.066(2)°, a:b:c 2.3252:1:2.5009, V 394.72(9) Å^3, $Z = 2$. Le groupe spatial est $P2_1/m$. La structure cristalline de la schlemaïte a été résolue par méthodes directes et affinée jusqu'à un résidu R de 4.8% en utilisant 1303 réflexions observées et mesurées avec un diffractomètre à quatre cercles équipé d'un détecteur de type CCD. La structure se compose de couches ordonnées et désordonnées intercalées. La couche ordonnée se compose d'échelles de $Pb^{2+} + Bi^{3+}$ coordonnées par Se, cette dernière démontrant de forts effets de paire stéréoactive isolée, et un réseau de Cu^+ coordonné par des anions de Se. La couche désordonnée se compose d'une rangée de sites en partie occupés par Cu^+ et Ag^+ dans une variété de coordinences, et un agencement ordonnée à courte échelle. Les sept raies les plus intenses du spectre de diffraction X [d en Å(I)(*hkl*)] sont: 3.189(100)(012), 3.132(100)$(\bar{1}12)$, 2.601(70)$(\bar{1}13)$, 2.505(50)$(\bar{3}11)$, 2.151(60)(014), 2.058(80)(020) et 1.909(50)$(\bar{3}14)$. Le nom de la nouvelle espèce rappelle le bassin minier Schlema–Alberoda, près de Schneeberg, dans l'ancienne région minière de la Saxe, Allemagne.

Mots-clés: schlemaïte, nouvelle espèce minérale, séléniure de Cu–Pb–Bi, eucairite, berzélianite, données à la microsonde électronique, données de réflectivité, structure cristalline, données de diffraction X, Niederschlema–Alberoda, Erzgebirge, Allemagne.

INTRODUCTION

Of the three vein-type uranium deposits in the Schneeberg – Schlema – Alberoda ore district (*i.e.*, Schneeberg, Oberschlema, Niederschlema–Alberoda), Niederschlema–Alberoda is considered the major occurrence of selenides in the Erzgebirge of Germany. Selenide minerals occur mainly as nests (2–5 cm in diameter) and fracture fillings in dolomite – ankerite – (calcite) veins, and as disseminated grains in intergranular spaces in the Fe–Mg carbonates.

In a current investigation of Se-bearing minerals from Niederschlema–Alberoda, a variety of rare selenides of Cu, Bi, Hg, Ni and other elements were discovered (these will be reported elsewhere). In addition to these rare selenides, we discovered some new Se-bearing species. One of these new species, a Cu–Pb–Bi selenide of composition $(Cu,\square)_6(Pb,Bi)Se_4$, is the subject of this paper.

The new mineral is named *schlemaite* after the Schlema–Alberoda ore field in the ancient mining region of Saxony, Germany. The mineral and mineral name have been approved by the Commission on New Minerals and Mineral Names, IMA (2003–26). Type material (polished section F2) is deposited at the Natural History Museum, London, U.K., as BM 2003,4. The type ore sample (S477), from which section F2 was made, will be archived at the Mineralogical Institute of the Technische Universität Bergakademie Freiberg, Germany, under the inventory number 80824. A single-crystal mount and a powder mount are housed in the Systematic Reference Series of the National Mineral Collection of Canada, Geological Survey of Canada, Ottawa (catalogue number 68099).

OCCURRENCE AND ASSOCIATED MINERALS

Schlemaite occurs at Niederschlema–Alberoda (lat. 50°37'N, long. 12°40'E), a vein-type uranium deposit near the town of Hartenstein, western Erzgebirge, Saxony, Germany. Type sample S477 was collected in 1960 from the "Tiber" dike, on the –855-m level, block 5128, near the main shaft (No. 371). The associated minerals in polished section F2 made from sample S477, which contains the schlemaite grain used for optical, physical and crystallographic measurements (F2), include clausthalite, eucairite, berzelianite and löllingite in a dolomite–ankerite matrix. Another schlemaite-bearing polished section (F2/1) from the type ore sample contains in addition tiemannite, umangite and bohdanowiczite.

The first detailed mineralogical and paragenetic studies of the selenide assemblages (Harlass & Schützel 1965, Ryschow 1972) were followed up with electron-microprobe studies (Dymkov *et al.* 1982, 1989, 1991, Förster & Tischendorf 2001, Förster *et al.* 2002). The selenium-bearing minerals reported from Niederschlema–Alberoda include: clausthalite (PbSe), tiemannite (HgSe), naumannite (Ag_2Se), klockmannite (CuSe), umangite (Cu_3Se_2), berzelianite ($Cu_{2-x}Se$), bukovite ($Cu_3FeTl_2Se_4$), permingeatite (Cu_3SbSe_4), crookesite (Cu_7TlSe_4), eucairite (AgCuSe), mgriite [$(Cu,Fe)_3AsSe_3$], and mercurian giraudite [$Cu_{10}(Hg,Cu)_2As_4Se_{13}$]–hakite [$Cu_{10}(Hg,Cu)_2Sb_4Se_{13}$] solid solutions.

Appearance and Physical Properties

Schlemaite is usually intergrown with berzelianite, eucairite and clausthalite to form aggregates up to several hundred micrometers across (Figs. 1, 2). It also occurs as isolated crystals up to a few hundred micrometers in length. The anhedral to subhedral grains show no obvious forms or twinning. Schlemaite is black and opaque with a metallic luster and black streak. It is brittle, with an uneven fracture and no obvious cleavage. Schlemaite has a polishing hardness greater than that of coexisting clausthalite, berzelianite and eucairite. The Vickers hardness number (VHN) for a 25 g load is 106 kg/mm^2 (range 92–116, five indentations), the indentations being perfect to slightly fractured. This VHN roughly equates to a Mohs hardness of 3 and is significantly higher than that determined for clausthalite, berzelianite and eucairite (respectively, VHN_{100} 44–49, VHN_{100} 21–24, and VHN_{25} 27–31; QDF3, Criddle & Stanley 1993). The density could not be measured because of the small grain-size and dearth of pure material. Calculated on the basis of the mean chemical composition and unit-cell parameters derived from crystal-structure refinement, the density is 7.74 (cations normalized to 11 atoms per formula unit, *apfu*) or 7.54 g/cm^3 (cations normalized to 4 Se atoms) for $Z = 2$.

Optical Properties

The sample containing schlemaite was prepared for optical investigation and measurement using standard diamond polishing techniques (Stanley & Laflamme 1998).

In plane-polarized reflected light (from an unfiltered quartz–halogen lamp at about 3100 K), schlemaite is grey, with very weak bireflectance and no reflectance pleochroism. However, against the strong blue color of the associated berzelianite, schlemaite appears slightly pink in this association with clausthalite (white) and

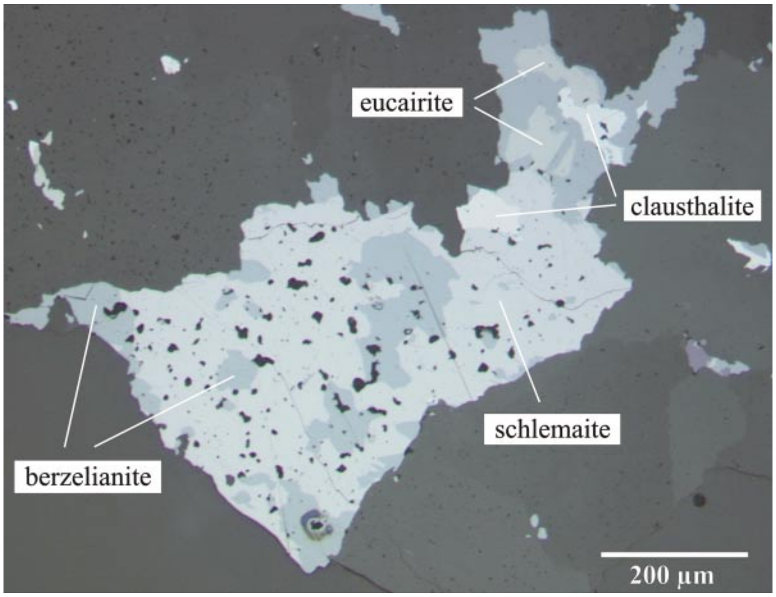

FIG. 1. Reflected-light digital-image of the intermixed schlemaite grain in type sample F2, from which the reflectance, crystallographic and crystal-structure data were obtained.

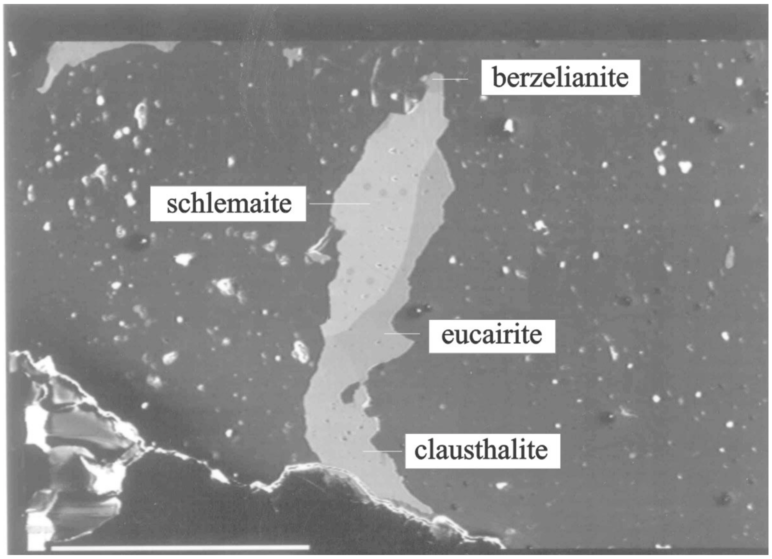

FIG. 2. Secondary-electron image of a polymineralic aggregate composed of schlemaite, eucairite, clausthalite and berzelianite (cotype sample F2/1). Scale bar: 200 μm.

eucairite (beige). Under crossed polars, schlemaite has very weak anisotropy, with rotation tints in shades of very pale metallic orange and blue, and no internal reflections. Digital photomicrographs were taken using a JVC KY–F7OU 3CCD camera mounted on a Zeiss Axioplan microscope equipped with Synoptics image-capturing software.

Reflectance measurements were made relative to a WTiC reflectance standard (Zeiss 314) with a Zeiss MPM800 microspectrophotometer. The objectives used in air and in oil (Zeiss West Germany, immersion oil 518C DIN 58.884; measurements were undertaken at 21°C) had magnifying powers of ×50, and constant effective numerical apertures were obtained in the two media by adjustment of the illuminator-aperture diaphragm. The bandwidth of the grating monochromator was set to 5 nm, and intensity data were collected at an interval of 10 nm from 400 to 700 nm. The weak anisotropy made it difficult to orient the measured grains at their extinction positions, but these were checked photometrically for maxima and minima. Intensity data were collected from five spectral scans at each of the four orthogonal "extinction" positions, and R_1 (lower) and R_2 (higher) data were calculated relative to the intensity values of the WTiC standard. Table 1 includes representative reflectance and color values for schlemaite. The reflectance curves in air for schlemaite and furutobeite, $(Cu,Ag)_6PbS_4$, are given in Figure 3.

CRYSTAL STRUCTURE

Single-crystal X-ray data

Crystal-structure intensity data were collected with a Bruker *P*4 four-circle diffractometer equipped with a SMART 1K CCD detector and Mo$K\alpha$ X-radiation on a crystal 5 × 40 × 40 μm. A total of 6719 reflections were collected and processed according to the procedure of Cooper & Hawthorne (2001). The unit cell was determined by least-squares refinement based on 2000 reflections with $I > 10\ \sigma I$, giving the following values: *a* 9.5341(8), *b* 4.1004(3), *c* 10.2546(8) Å, β 100.066(2)°, *V* 394.72(9) Å^3, *a:b:c* 2.3252:1:2.5009. Schlemaite is monoclinic and has the space group $P2_1/m$. The crystal structure was solved by direct methods and refined to an *R* index of 4.8% and a *wR* index of 5.4%. A summary of the miscellaneous data about the crystal is given in Table 2. Atom positions and displacement factors are given in Table 3, selected interatomic distances are given in Table 4, and refined site-scattering values and assigned site-populations are given in Table 5. Observed and calculated structure-factors may be obtained from the Depository of Unpublished Data, CISTI, National Research Council, Ottawa, Ontario K1A 0S2, Canada.

Description of the site

The structure can be conveniently divided into two parts, an *ordered part* and a *disordered part*. In the *or-*

dered part of the structure, there are four *Se* sites, each of which is fully occupied by Se; hence the formula of the crystal was normalized on 4 Se *apfu*. The closest Se–Se approach is 3.67 Å.

There is a single *Pb* site occupied by 0.61 Pb + 0.39 Bi (Table 5). Pb and Bi have very similar X-ray scattering-factors, and a site-occupancy refinement cannot provide a quantitative measure of Pb relative to Bi. On one side of the Pb site, there are three short bonds to Se(1) (<2.87 Å>), and on the other side, five long bonds to Se atoms (<3.40 Å>) (Table 4). The extremely asymmetrical distribution in bond lengths about the *Pb* site is characteristic of stereoactive lone-pair behavior of the Pb^{2+} and Bi^{3+} ions. The empirical radii for [8]-coordinated Pb^{2+} and Bi^{3+} are 1.29 and 1.17 Å, respectively (Shannon 1976), and when combined with the 1.98 Å radius of Se^{2+}, the resulting <Pb^{2+}–Se> and <Bi^{3+}–Se> distances are 3.27 and 3.15 Å, respectively. The observed composition derived from electron-microprobe analyses ($Pb_{0.61}Bi_{0.39}$) gives a predicted aggregate <Pb,Bi–Se> distance of 3.22 Å, in close agreement with the observed value of 3.20 Å (Table 4).

TABLE 1. REFLECTANCE DATA AND COLOR VALUES FOR SCHLEMAITE

λ	R_1	R_2	$^{im}R_1$	$^{im}R_2$
400 nm	35.3 %	36.2 %	20.6 %	21.7 %
420	36.1	37.1	20.9	22.3
440	36.3	37.65	21.1	22.7
460	36.6	38.0	21.1	23.0
480	36.6	38.1	21.05	23.1
500	36.5	38.1	20.8	22.9
520	36.4	38.1	20.7	22.8
540	36.5	38.1	20.7	22.8
560	36.4	38.2	20.7	22.8
580	36.55	38.2	20.9	22.9
600	36.7	38.35	21.0	23.1
620	36.7	38.4	21.1	23.1
640	36.7	38.5	21.0	23.2
660	36.6	38.4	21.1	23.2
680	36.7	38.4	21.1	23.2
700	36.4	38.5	21.0	23.4
470	36.6	38.1	21.1	23.0
546	36.45	38.1	20.7	22.8
589	36.6	38.3	20.95	22.9
650	36.6	38.5	21.0	23.2
Color Values		A illuminant		
x	0.448	0.449	0.448	0.449
y	0.408	0.408	0.406	0.407
Y%	36.6	38.2	20.9	22.9
λ_d	591	585	c537	616
P_e%	0.5	1.1	0.5	0.5
		C illuminant		
x	0.311	0.311	0.310	0.311
y	0.317	0.318	0.315	0.317
Y%	36.5	38.2	20.8	22.9
λ_d	578	574	c536	585
P_e%	0.4	0.1	0.6	0.5

Site-occupancy refinement for the *Cu*(1) and *Cu*(2) sites gave full occupancy of each site by Cu. The *Cu*(1) site is tetrahedrally coordinated by four Se atoms, and the *Cu*(2) site is coordinated by three Se atoms in a triangular configuration, with the *Cu*(2) site slightly out of the plane. The bond-valence sums at the *Cu*(1) and *Cu*(2) sites are 0.93 and 0.95 valence units (*vu*), respectively, consistent with Cu^{1+} at each site (Table 4).

In the *disordered part* of the structure, the *Cu*(3) and *Cu*(8) sites are occupied by 0.54 and 0.26 Cu atoms, respectively (Table 5), and are separated by 0.48(6) Å. The *Cu*(3) site is tetrahedrally coordinated, whereas the *Cu*(8) position is in triangular coordination. The *Cu*(8)–Se(1) distance, at 2.80 Å, is too long for any appreciable interaction (*i.e.,* ~0.1 *vu*), in accord with the bond-valence sum (1.03 *vu*) at *Cu*(8).

The *Cu*(4) and *Cu*(7) sites are occupied by 0.92 and 0.07 Cu atoms, respectively (Table 5); *Cu*(4)–*Cu*(7) is equal to 0.74(7) Å, and *Cu*(4)–*Cu*(4), to 0.63(2) Å. The *Cu*(4) site is coordinated by three Se atoms. The *Cu*(7) site is coordinated by only two Se atoms in near-linear geometry [Se(2)–*Cu*(7)–Se(4) = 1.66(4) Å].

The *Cu*(5), *Cu*(6) and *Ag* sites are occupied by 0.96 Cu, 0.18 Cu and 0.40 Ag, respectively (Table 5). All three sites have distorted triangular coordination. The positional disorder involving these three sites is rather complicated. Of all the disordered sites, *Cu*(5) has the largest occupancy factor [0.96(3) *apfu* Cu], and possibly is fully occupied [*note*: only half of the general positions can be simultaneously occupied owing to close *Cu*(5)–*Cu*(5) approaches]. Full (allowed) occupancy of the *Cu*(5) site would allow up to half of the *Ag* sites to be occupied, placing an upper limit of 0.5 Ag *apfu* on the composition. The <*Ag*–Se> distance is 2.62 Å, appreciably longer than <*Cu*–Se> distances for *Cu* sites that are coordinated by three Se atoms. Using the bond-valence curve for Ag–Se (Brese & O'Keeffe 1991) gives a bond-valence sum at the *Ag* site of 1.15 *vu*, whereas the corresponding value for a Cu–Se interaction gives a sum of only 0.61 *vu*. We can therefore safely conclude that the majority of the scattering at the *Ag* site is due to Ag.

Structural connectivity

In the *ordered part*, each *Pb* site is coordinated by three Se(1) sites, and each Se(1) site, in turn, by three *Pb* sites, to form a Pb–Se ladder that extends parallel to the *b* axis (Fig. 4a). The [4]-coordinated *Cu*(1) and [3]-coordinated *Cu*(2) sites link through Se(2) and Se(3) sites to form a corrugated Cu–Se network that extends along the *b* axis (Fig. 4b).

In the *disordered part,* the *Cu*(3,4,5,6,7,8) and *Ag* sites form complex disordered layers [parallel to (100) and centered at $x \approx ½$] that alternate with ordered Pb–Se ladders and corrugated *Cu*(1,2)–Se(2,3) slabs centered at $x \approx 0$ (Fig. 5).

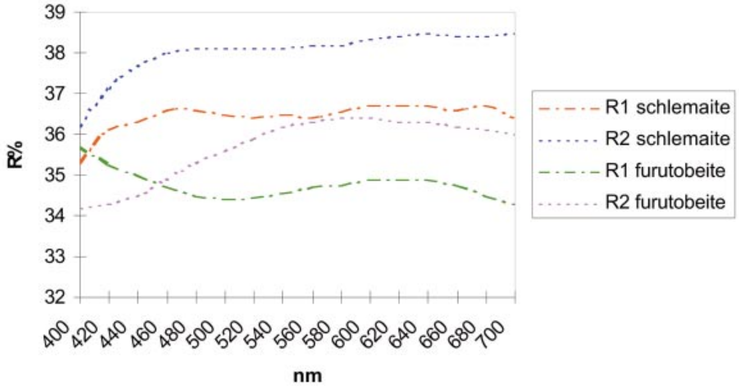

FIG. 3. Reflectance curves for schlemaite and furutobeite (Sugaki *et al.* 1981) in air.

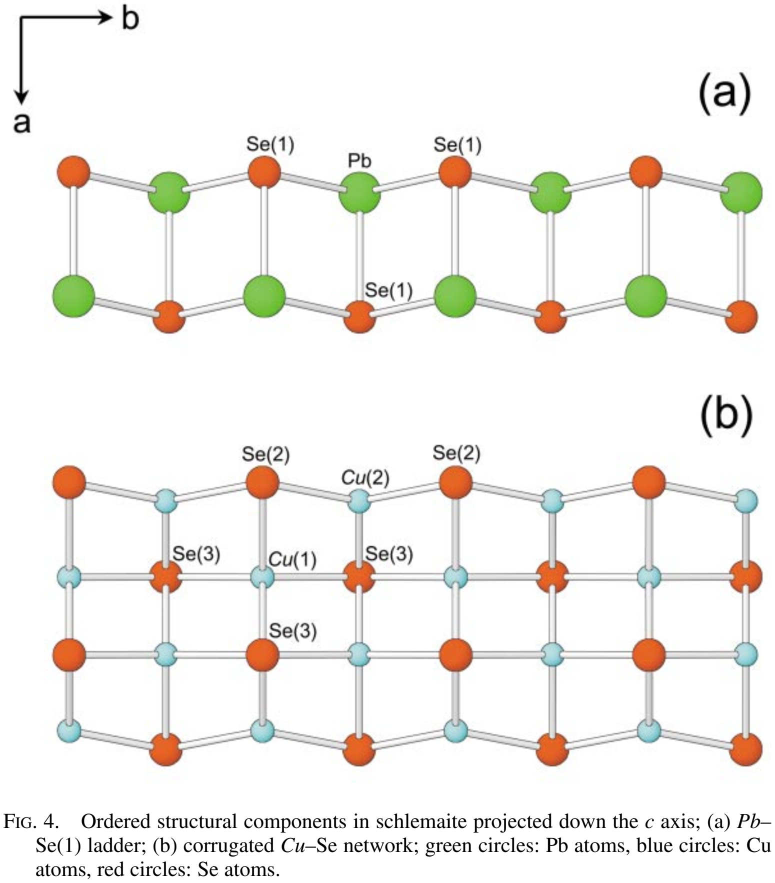

FIG. 4. Ordered structural components in schlemaite projected down the *c* axis; (a) *Pb*–Se(1) ladder; (b) corrugated *Cu*–Se network; green circles: Pb atoms, blue circles: Cu atoms, red circles: Se atoms.

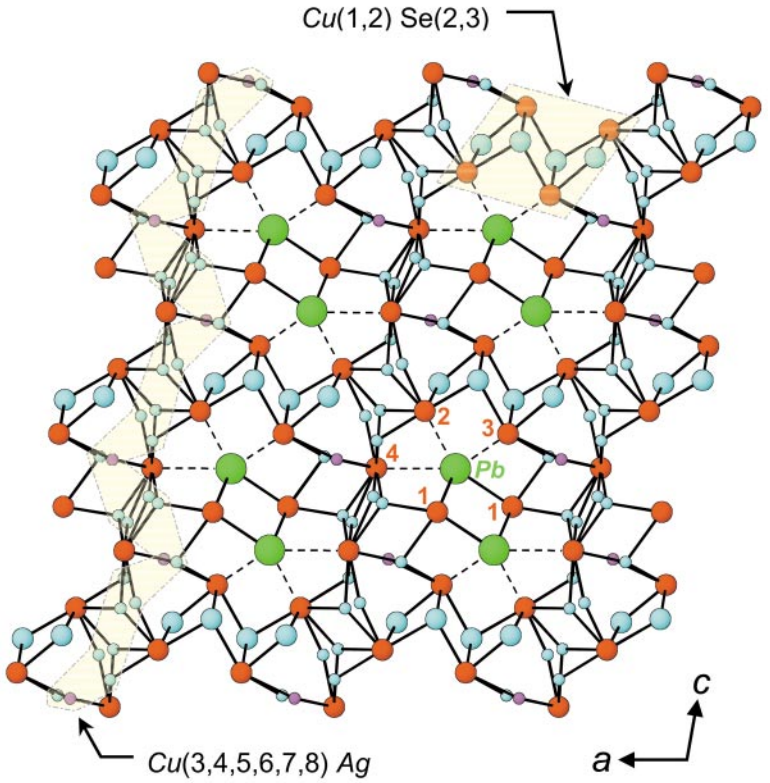

FIG. 5. The crystal structure of schlemaite projected down the *b* axis; legend as in Figure 4. Larger blue and red circles correspond to fully ordered *Cu* and Se sites, respectively, and the smaller circles, to the disordered sites. An ordered *Cu*(1,2)–Se(2,3) gridwork and disordered *Cu*(3,4,5,6,7,8) *Ag* layer (100) is highlighted with yellow shading. Red numbers are Se site labels. Dashed Pb–Se bonds are long bonds.

X-ray powder-diffraction data

X-ray powder-diffraction data (Table 6) were obtained from the area of the sample adjacent to that from which the single-crystal fragment was dug out. Unit-cell parameters were refined on 23 powder reflections between 4.822 and 1.677 Å for which unambiguous indexing, based on visual inspection of single-crystal precession photographs, was possible. The refined unit-cell parameters from powder data are *a* 9.529(4), *b* 4.115(2), *c* 10.237(5) Å, β 100.29(5)°, *V* 394.9(9) Å^3, *a*:*b*:*c* 2.3157:1:2.4877. The powder-diffraction data are unique and are not similar to any other phase listed in the Powder Diffraction File. The PSC (Pearson Symbol Code) for schlemaite (simplified formula) is *mP* 22, and the mineral seems to have a unique prototype structure.

TABLE 2. MISCELLANEOUS INFORMATION FOR THE CRYSTAL-STRUCTURE DETERMINATION OF SCHLEMAITE

a (Å)	9.5341(8)	crystal size (μm)	5 x 40 x 40 μm
b	4.1004(3)	radiation	Mo$K\alpha$
c	10.2546(8)	No. of reflections	6719
β (°)	100.066(2)		
V (Å^3)	394.72(9)	No. in Ewald sphere	4105
Sp. Gr.	$P2_1/m$	No. unique reflections	1303
Z	2	No. $\lvert F_o\rvert > 5\sigma(\lvert F\rvert)$	813
D_{calc} (g/cm^3)	7.54	R_{merge} %	2.6
		R(obs) %	4.8
		wR(obs) %	5.4
Cell content	2 [$(Cu^{1+},Ag^{1+})_{\Sigma 5.69}$ $(Pb^{2+}_{0.61}\ Bi^{3+}_{0.39})$ Se_4]		

$R = \Sigma(\lvert F_o\rvert - \lvert F_c\rvert) / \Sigma\lvert F_o\rvert$

$wR = [\Sigma w(\lvert F_o\rvert - \lvert F_c\rvert)^2 / \Sigma wF_o^2]^{½}$, $w = 1$

CHEMICAL COMPOSITION

Schlemaite and the associated selenides were analyzed for Ag, Hg, Cu, Fe, Co, Ni, Zn, Cd, Pb, Pd, Pt, Sb, As, Bi, Te, S and Se. Chemical analyses were obtained at the GeoForschungsZentrum, Potsdam, using an automated Cameca CAMEBAX SX–50 electron microprobe operated in wavelength-dispersion mode. The operating conditions were as follows: accelerating voltage 20 kV, beam current 40 nA, and beam diameter 1–2 μm. The counting times on the peak were 50 s, and 25 s for background counts on each side of the peak. Data reduction was done with a PAP correction procedure (Pouchou & Pichoir 1985).

Lines measured were $K\alpha$ for Fe, Co, Ni, Cu, Zn, Se and S, $K\beta$ for As, $L\alpha$ for Hg, Pd, Pt, Cd, Sb, Te, and Ag and As in schlemaite, $L\beta$ for Ag, $M\alpha$ for Bi and Pb (schlemaite), and $M\beta$ for Pb. Primary standards included pure metals for Co, Pd, and Pt, chalcopyrite for Fe, Cu, and S, pentlandite for Ni, sphalerite for Zn, cinnabar for Hg, galena for Pb, GaAs for As, Bi_2Se_3 for Bi and Se, Ag_2Te for Ag and Te, InSb for Sb, and CdS for Cd.

Electron-microprobe data for schlemaite are given in Table 7. We report (a) the mean analytical results obtained for the schlemaite grain in polished section F2 used for the physical, optical and X-ray studies, (b) results of additional electron-microprobe analyses of schlemaite illustrating a greater range in composition, and (c) representative results of individual analyses.

TABLE 3. ATOM POSITIONS AND DISPLACEMENT FACTORS FOR SCHLEMAITE

Site	x	y	z	U_{eq}	U_{11}	U_{22}	U_{33}	U_{23}	U_{13}	U_{12}
Pb	0.1178(1)	1/4	0.6702(1)	0.0354(5)	0.0460(8)	0.0220(6)	0.0425(8)	0	0.0200(6)	0
Ag	0.3457(8)	1/4	0.2912(9)	0.054(3)	0.035(4)	0.057(6)	0.061(5)	0	-0.017(3)	0
Cu(1)	-0.0872(5)	1/4	-0.0409(4)	0.035(1)	0.048(2)	0.020(2)	0.042(2)	0	0.018(2)	0
Cu(2)	0.2588(4)	1/4	0.0273(4)	0.034(1)	0.044(2)	0.023(2)	0.043(2)	0	0.026(2)	0
Cu(3)	0.583(3)	1/4	0.474(2)	0.024(4)	0.013(8)	0.036(4)	0.024(6)	0	0.005(5)	0
Cu(4)	0.500(1)	0.327(2)	-0.0849(7)	0.044(3)	0.038(5)	0.056(8)	0.034(3)	-0.001(3)	-0.004(3)	0.014(4)
Cu(5)	0.7127(7)	0.075(2)	0.7208(8)	0.062(3)	0.038(4)	0.083(6)	0.065(5)	0.039(4)	0.012(3)	0.029(4)
Cu(6)	0.509(2)	1/4	0.212(2)	0.018(6)						
Cu(7)	0.561(8)	1/4	0.891(5)	0.010(2)						
Cu(8)	0.537(7)	1/4	0.446(4)	0.036(7)						
Se(1)	0.1650(3)	3/4	0.4887(3)	0.0179(7)	0.018(1)	0.019(1)	0.017(1)	0	0.004(1)	0
Se(2)	0.3008(3)	3/4	-0.0880(2)	0.0171(7)	0.018(1)	0.017(1)	0.017(1)	0	0.0058(9)	0
Se(3)	0.0883(3)	1/4	0.1837(3)	0.0188(8)	0.024(1)	0.017(1)	0.017(1)	0	0.009(1)	0
Se(4)	0.5289(3)	3/4	0.3268(3)	0.0238(8)	0.024(1)	0.030(1)	0.020(1)	0	0.009(1)	0

TABLE 4. SELECTED INTERATOMIC DISTANCES (Å) AND BOND VALENCES (*vu*) IN SCHLEMAITE

Pb-Se(1),a	x2	2.857(2)	0.64	*Cu*(4)-Se(2)		2.570(9)	0.23
Pb-Se(1)b		2.896(3)	0.57	*Cu*(4)-Se(2)f		2.380(8)	0.38
Pb-Se(2)d,e	x2	3.447(2)	0.13	*Cu*(4)-Se(4)f		2.467(7)	0.30
Pb-Se(3)b,h	x2	3.367(3)	0.16	<*Cu*(4)-Se>		2.472	0.91
Pb-Se(4)c		3.363(3)	0.16				
<*Pb*-Se>		3.200	2.59	*Cu*(5)-Se(1)c		2.714(9)	0.15
				Cu(5)-Se(3)j		2.384(8)	0.37
Ag-Se(3)		2.509(8)	0.51	*Cu*(5)-Se(4)c		2.380(7)	0.38
Ag-Se(4),a	x2	2.676(5)	0.32	<*Cu*(5)-Se>		2.493	0.90
<*Ag*-Se>		2.620	1.15				
				Cu(6)-Se(2)f		2.40(2)	0.36
Cu(1)-Se(2)g		2.614(5)	0.20	*Cu*(6)-Se(4),a	x2	2.35(2)	0.41
Cu(1)-Se(3)		2.600(5)	0.21	<*Cu*(6)-Se>		2.37	1.18
Cu(1)-Se(3)g,i	x2	2.518(3)	0.26				
<*Cu*(1)-Se>		2.563	0.93	*Cu*(7)-Se(2)c		2.21(5)	0.60
				Cu(7)-Se(4)c		2.25(5)	0.54
Cu(2)-Se(2),a	x2	2.434(3)	0.33	<*Cu*(7)-Se>		2.23	1.14
Cu(2)-Se(3)		2.476(5)	0.29				
<*Cu*(2)-Se>		2.448	0.95	*Cu*(8)-Se(4),a	x2	2.38(2)	0.38
				Cu(6)-Se(4)c		2.51(5)	0.27
Cu(3)-Se(1)c		2.37(3)	0.39	<*Cu*(6)-Se>		2.42	1.03
Cu(3)-Se(4),a	x2	2.54(1)	0.25				
Cu(3)-Se(4)c		2.47(2)	0.30				
<*Cu*(3)-Se>		2.48	1.19				

a: $x, y - 1, z$; b: $\bar{x}, \bar{y} + 1, \bar{z} + 1$; c: $\bar{x} + 1, \bar{y} + 1, \bar{z} + 1$; d: $x, y, z + 1$; e: $x, y - 1, z + 1$; f: $\bar{x} + 1, \bar{y} + 1, \bar{z}$; g: $\bar{x}, \bar{y} + 1, \bar{z}$; h: $\bar{x}, \bar{y}, \bar{z} + 1$; i: $\bar{x}, \bar{y}, \bar{z}$; j: $\bar{x} + 1, \bar{y}, \bar{z} + 1$.

TABLE 5. REFINED SITE-SCATTERING VALUES (*epfu*) AND ASSIGNED SITE-POPULATIONS (*apfu*) FROM STRUCTURE REFINEMENT (SREF), PLUS CORRESPONDING VALUES FROM ELECTRON-MICROPROBE ANALYSES (EMPA)

Site	SREF *epfu*	SREF *apfu*	EMPA *epfu*	EMPA *apfu*
		ordered		
Pb	83.7(7)	–	82.4	0.61 Pb + 0.39 Bi
Cu(1)	29	1 Cu	29	1 Cu
Cu(2)	29	1 Cu	29	1 Cu
		disordered		
Cu(3)	16(2)	0.54(7) Cu	99.5	3.43
Cu(4)	26.7(9)	0.92(3) Cu		
Cu(5)	27.9(7)	0.96(3) Cu		
Cu(6)	5.3(4)	0.18(1) Cu		
Cu(7)	1.9(8)	0.07(3) Cu		
Cu(8)	7(2)	0.26(7) Cu		
Ag	18.9(6)	0.40(1) Ag	12.2	0.26
Σ	104(7)	3.3(3)	111.7	3.69

Representative compositions of metallic minerals associated with schlemaite in polished section F2 are given in Table 8.

The data in Table 7 show that Cu, Ag, Pb, Bi and Se are consistently present in schlemaite, whereas Au, Hg, Cd, Fe and S occasionally occur at concentrations of a few tenths of a weight percent. The concentrations of Co, Ni, Zn, Pd, Pt, As, Sb and Te were found to be below their detection limits, between 0.02 and 0.04 wt.%. The empirical formula for schlemaite is $(Cu_{5.65}Ag_{0.22})_{\Sigma 5.87}(Pb_{0.61}Bi_{0.40})_{\Sigma 1.01}Se_{4.11}$, based on 11 atoms per formula unit (*apfu*). Normalization to 4 Se *apfu* gives $(Cu_{5.50}Ag_{0.21})_{\Sigma 5.71}(Pb_{0.60}Bi_{0.39})_{\Sigma 0.99}Se_4$. The 13 grains investigated (73 analyses) all contain Pb > Bi and give a mean composition of $(Cu_{5.43}Ag_{0.26})_{\Sigma 5.69}$ $(Pb_{0.61}Bi_{0.39})_{\Sigma 1.00}$ Se_4 or $(Cu_{5.59}Ag_{0.26})_{\Sigma 5.85}$ $(Pb_{0.62}Bi_{0.40})_{\Sigma 1.02}$ $Se_{4.12}$. Crystal-structure analysis indicates that all bond lengths and associated bond-valence sums are consistent with Cu^{1+} and Ag^{1+} in combination with Pb^{2+} and Bi^{3+}. The end-member compositions are $Cu^{1+}{}_6Pb^{2+}Se_4$ (schlemaite) and $Cu^{1+}{}_5Bi^{3+}Se_4$ (unnamed). Relative to the Pb^{2+} end-member, the Bi^{3+} end-member contains one less Cu^{1+} atom. In schlemaite, three strong bonds are directed toward the Se atom at Se(1) by (Pb,Bi) atoms. The incident bond-valence at the Se(1) site will differ appreciably between the Pb^{2+} and Bi^{3+} end-members, and we can examine the local bonding at the Se(1) site in order to identify a mechanism by which the bond-valence requirements of the Se atom are satisfied. Other bonds to Se(1) are from Cu^{1+} atoms at the disordered *Cu*(3) and *Cu*(5) sites. The environment about Se(1) is shown in Figure 6; the *Cu*(3) and *Cu*(5) positions are not mutually interfering. The configuration for the intermediate composition studied here is shown in Figure 6a. The *Cu*(3)–Se(1) bond is shorter (and hence stronger) than the *Cu*(5)–Se(1) bond; the *Cu*(5) site is nearly fully occupied, whereas the *Cu*(3) site contains significant vacancy. The sites shown in Figure 6 collectively contribute 1 *apfu*, and the relative fraction of Pb^{2+} at the *Pb* site is in close agreement with the fraction of Cu^{1+} at the *Cu*(3) site. This agreement suggests that the $Bi^{3+} \leftrightarrow Pb^{2+}$ substitution is coupled to a $\square \leftrightarrow Cu^{1+}$ substitution at the *Cu*(3) site. The local arrangements for the Pb and Bi end-members are shown in Figures 6b and 6c, respectively. Considering the overall presence of significant Bi in the grains from Niederschlema–Alberoda, the simplified formula of schlemaite can be written as $(Cu,\square)_6(Pb,Bi)Se_4$. End-member schlemaite Cu_6PbSe_4 requires: Cu 42.16, Pb 22.92, Se 34.92, total 100.0 wt.% (Table 7).

TABLE 6. X-RAY POWDER-DIFFRACTION DATA FOR SCHLEMAITE

	I_{est}	d_{meas}Å	d_{calc}Å	*hkl*		I_{est}	d_{meas}Å	d_{calc}Å	*hkl*
	5	4.822	4.809	$\bar{1}02$		25	2.374	2.379	$\bar{4}01$
	30	4.575	4.574	$\bar{2}01$				2.369	$\bar{3}12$
	10	4.123	4.139	102	*	5	2.335	2.340	311
	5	3.982	3.986	201	*	60	2.151	2.148	014
	40	3.802	3.809	011	*	40	2.116	2.115	312
			3.785	$\bar{2}02$	*	5	2.074	2.076	$\bar{2}14$
*	10	3.360	3.358	003	*	80	2.058	2.058	020
	100	3.189	3.187	012		10	2.021	2.028	114
*	100	3.132	3.127	$\bar{1}12$				2.015	005
	10	3.001	2.996	103	*	10	1.984	1.984	$\bar{2}05$
			2.995	$\bar{2}03$	*	50	1.909	1.911	$\bar{3}14$
*	30	2.903	2.898	$\bar{3}02$	*	20	1.875	1.875	500
*	10	2.862	2.863	211	*	30	1.850	1.849	214
*	70	2.788	2.786	$\bar{2}12$	*	5	1.831	1.832	$\bar{1}15$
*	70	2.601	2.601	$\bar{1}13$		5	1.808	1.809	015
*	50	2.505	2.500	$\bar{3}11$				1.809	304
*	10	2.460	2.466	302	*	10	1.779	1.778	$\bar{5}03$
	40	2.425	2.422	113		3	1.755	1.754	023
			2.421	$\bar{2}13$		3	1.722	1.724	222
	20	2.404	2.405	$\bar{2}04$	*	15	1.702	1.702	$\bar{5}12$
					*	15	1.677	1.678	$\bar{3}22$

Debye–Scherrer powder camera 114.6 mm in diameter; Cu radiation, Ni-filter (λ Cu$K\alpha$ = 1.54178 Å). Intensities estimated visually; the pattern was not corrected for shrinkage and had no internal standard. * : reflections selected for unit-cell refinement. Indexed on *a* 9.529, *b* 4.115, *c* 10.237 Å, β 100.29°.

Among the metallic minerals intimately associated with schlemaite, there is minor substitution of Cu, Ag, Au, Hg, Fe and Bi for Pb in clausthalite (Table 8). Copper and Bi may be present at concentrations greater than 1 wt.%. Berzelianite may contain small amounts of Ag, Hg, Pb, Fe and S. Eucairite has a composition close to

TABLE 7. ELECTRON-MICROPROBE DATA (WT.%) FOR SCHLEMAITE AND THEORETICAL END-MEMBER COMPOSITIONS

	Grain extracted			All grains			Representative point analyses						schlemaite	unnamed	furutobeite
	Average[1]	STDW	Range	Average[2]	STDW	Range							Cu_6PbSe_4	Cu_5BiSe_4	Cu_6PbS_4
Cu	38.86	0.51	37.86 – 39.90	38.40	1.59	35.78 – 41.09	39.97	41.09	39.90	39.65	36.45	35.78	42.16	37.71	53.19
Ag	2.57	0.39	1.83 – 3.36	3.02	1.38	0.18 – 5.21	0.18	0.98	1.83	2.81	4.73	5.21			
Au	0.07	0.07	0.00 – 0.21	0.07	0.07	0.00 – 0.24		0.19	0.11	d.l.	d.l.	d.l.			
Hg	0.09	0.10	0.00 – 0.25	0.05	0.08	0.00 – 0.30	d.l.	d.l.	d.l.	d.l.	d.l.	0.11			
Pb	13.75	0.25	13.41 – 14.41	13.96	0.36	13.06 – 14.86	13.36	14.37	13.91	13.95	14.66	13.71	22.92		28.90
Cd	d.l.			d.l.		0.00 – 0.10	d.l.	d.l.	d.l.	d.l.	d.l.	d.l.			
Fe	d.l.			d.l.		0.00 – 0.07	0.07	d.l.	d.l.	d.l.	d.l.	0.05			
Bi	9.12	0.41	8.10 – 9.72	9.10	0.68	7.41 – 10.58	10.51	8.72	9.44	7.69	8.29	9.85		24.80	
S	d.l.			d.l.		0.00 – 0.09	0.09	d.l.	d.l.	d.l.	d.l.	d.l.			17.91
Se	35.11	0.24	34.54 – 35.49	35.11	0.31	34.52 – 35.60	35.58	35.22	35.25	35.04	35.11	35.30	34.92	37.49	
Total	99.57			99.69			99.75	100.56	100.44	99.14	99.23	100.01	100	100	100

d.l.: below detection limit. Blank: not analyzed. [1]: average of 22 point determinations. [2]: average of 73 point determinations.

the ideal end-member, with insignificant substitutions of Hg, Pb, Fe and S. Minor amounts of Cu substituting for Fe and Se substituting for As characterize the composition of löllingite. These various substitutions indicate the compositional complexity of the fluids from which the metallic minerals crystallized (Cu, Ag, Pb, Bi and Se as major components).

RELATION TO OTHER SPECIES

Schlemaite is chemically similar, and also probably structurally related, to furutobeite, $(Cu,Ag)_6PbS_4$ (Sugaki *et al.* 1981). Both have a (Cu,Ag)/Pb ratio of 6:1 relative to four anions ($Z = 4$) and have monoclinic symmetry with a similar β angle. However, their unit cells and space groups are different. The cell volume for furutobeite is 1.92 times that for schlemaite, a result of a doubling of the *c* axis (schlemaite). We did not observe any evidence for a larger cell for schlemaite, and all (three-dimensional) spot intensities are uniform with no streaking. As all furutobeite compositions have a Cu/Ag ratio very close to 5:1, the structure of furutobeite, as yet undetermined, may contain an ordered distribution of Ag atoms. In summary, schlemaite is not isostructural with furutobeite and, thus, is not strictly the Se-analogue of furutobeite.

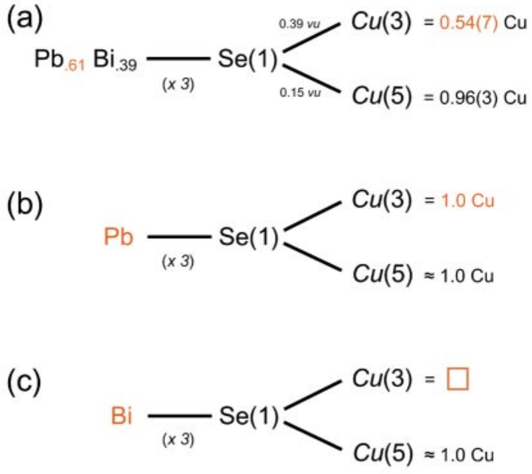

FIG. 6. The local bonding at the Se(1) site in schlemaite for: (a) the composition studied here; (b) the Pb end-member; (c) the Bi end-member.

TABLE 8. REPRESENTATIVE COMPOSITION OF METALLIC MINERALS ASSOCIATED WITH SCHLEMAITE IN SAMPLE F2

	Euc	Euc	Cls	Cls	Cls	Brz	Brz	Brz	Lol	Lol
Cu wt.%	25.62	25.63	1.32	0.75	d.l.	60.62	59.55	58.43	0.51	1.14
Ag	42.82	43.11	0.59	d.l.	0.42	0.10	d.l.	0.40	d.l.	d.l.
Au			0.12	d.l.						
Hg	0.03	d.l.	0.19	d.l.	d.l.	0.14	d.l.	0.18	0.02	0.02
Pb	0.08	d.l	69.21	72.03	71.77	d.l.	0.04	0.03	0.02	0.02
Fe	0.04	d.l.	0.19	d.l.	0.06	d.l.	0.19	0.06	26.85	26.50
As	d.l.	d.l.	d.l.	d.l.	d.l.	d.l.	d.l.	d.l.	69.97	69.47
Sb	d.l.	d.l.	d.l.	d.l.	d.l.	d.l.	d.l.	0.03	d.l.	d.l.
Bi	d.l.	0.07	d.l.	d.l.	1.03	d.l.	d.l.	d.l.	d.l.	d.l.
S	0.36	d.l.	d.l.	d.l.	d.l.	0.04	0.43	0.21		
Se	30.60	31.46	28.72	27.82	27.16	39.08	39.63	40.59	1.83	1.97
Total	99.54	100.28	99.88	100.59	100.43	99.99	99.90	99.92	99.19	99.13

d.l.: below detection limit. Blank: not analyzed. Euc: eucairite, Cls: clausthalite, Brz: berzelianite, Lol: löllingite.

CONDITIONS OF FORMATION

In the western Erzgebirge uranium deposits, three uraniferous vein-mineral associations can be distinguished: quartz – calcite – uraninite (*kku*), magnesian carbonate – uraninite – fluorite (*mgu*), and bismuth – cobalt – nickel ± silver ± uranium (*biconi*) (Schuppan *et al.* 1994, and references therein). Formation of the primary *kku* association took place during the early Permian (~270 Ma; Förster & Haack 1995). Colloform to reniform-botryoidal uraninite was deposited in veins, which also contain quartz, calcite, fluorite, coffinite, hematite, and sulfide minerals such as aikinite, galena, bismuthinite, chalcopyrite and pyrite. During the Jurassic (~190 Ma), oxidizing hydrothermal solutions overprinted and altered the early-formed veins and introduced new elements (Mg, Se, Pb, Ag). This mineralizing event gave rise to the *mgu* association. The bulk of the new components were probably mobilized from the metamorphic wallrocks (alteration haloes occur in felsic pelite, mica schist and gneiss, limestone, skarn, metadiabase, and mafic amphibolite). During this mobilization event, uraninite of Permian age was destabilized, and the uranium was redeposited as spherical aggregates of uraninite accompanied by dolomite, ankerite, fluorite, hematite and diverse sulfur-bearing (chalcopyrite, galena, bornite, tennantite) and selenium-bearing minerals. This association is most prominent at Niederschlema–Alberoda. Hydrothermal activity in response to tectonic processes in the early Cretaceous (~120 Ma) again gave rise to alteration of earlier-formed mineral assemblages (Förster & Haack 1995). Pre-existing uraninite and selenide minerals were partly corroded by infiltrating fluids and replaced by the telescoped *biconi* association, which comprises native elements (Ag, Bi, As), Co–Ni–Fe arsenides (skutterudite, safflorite, rammelsbergite, löllingite, nickeline) and Bi-bearing sulfides, together with recrystallized uraninite and coffinite. Quartz, fluorite, barite and siderite form the gangue of this association.

From the selenide assemblage, we can conclude that schlemaite is part of the *mgu* association of minerals. This origin is further supported by the composition of the associated löllingite, in which some Se substitutes for As. Löllingite of the later *biconi* association is virtually free of Se, but characteristically contains varying contents of S replacing As, and Ni and Co replacing Fe.

An accurate estimate of the P–T–X conditions of schlemaite formation is impossible without thermodynamic and fluid-inclusion data. End-member schlemaite has not yet been synthesized. The associated clausthalite and berzelianite have wide fields of stability in P–T–X space (Simon & Essene 1996), and the thermodynamic properties of eucairite are unknown. Tiemannite, umangite and bohdanowiczite have never been observed in intimate association with schlemaite and are not necessarily cogenetic with it. The presence of umangite could provide an important constraint on temperature and selenium fugacity during mineralization because it is stable only below 112°C, above which it decomposes to berzelianite and klockmannite (Chakrabarti & Laughlin 1981). At 100°C, a temperature commonly proposed for selenide mineralization associated with vein-type deposits, umangite crystallizes at $\log f(\mathrm{Se}_{2(g)})$ around –14.5 and at $\log f(\mathrm{S}_{2(g)}) < -23$ [assuming that $\log f(\mathrm{O}_{2(g)})$ is close to the hematite–magnetite buffer, –55.32; Simon *et al.* 1997]. Hematite forms an important constituent of the selenide assemblages at Niederschlema–Alberoda. However, whether these temperatures and the fugacities of Se and S also apply to the formation of schlemaite remains uncertain.

ACKNOWLEDGEMENTS

We are indebted to S. Flach (Damme, Germany), who has kindly provided the type sample of schlemaite from his private collection of selenium-bearing minerals. This sample, archived as S 477, is 6 × 5 × 3.5 cm in size and weighs 168 g. This sample was originally collected in 1964 by U. Lipp (deceased), who left it, together with numerous other selenide-bearing samples from Niederschlema–Alberoda, to S. Flach in 1996. We are also grateful to H. Schulz (Dresden, Germany), who donated the second schlemaite-bearing sample (Sh9) to HJF and GT. We thank D. Rhede and O. Appelt (GeoForschungsZentrum Potsdam) for their assistance with the electron-microprobe analyses. Constructive reviews from W. Paar (Salzburg, Austria) and D. Holstam (Stockholm, Sweden) and Associate Editor N.J. Cook, R.F. Martin and J.A. Mandarino helped to improve the manuscript. FCH was supported by a Canada Research Chair and by Major Equipment, Equipment, Discovery and Major Facilities Access grants from the Natural Sciences and Engineering Research Council of Canada.

REFERENCES

Brese, N.E. & O'Keeffe, M. (1991): Bond-valence parameters for solids. *Acta Crystallogr.* **B47**, 192-197.

Chakrabarti, D.J. & Laughlin, D.E. (1981): The Cu–Se (copper–selenium) system. *Bull. Alloy Phase Diagrams* **2**, 305-315.

Cooper, M.A. & Hawthorne, F.C. (2001): Structure topology and hydrogen bonding in marthozite, $\mathrm{Cu^{2+}\,[(UO_2)_3\,(SeO_3)_2\,O_2]\,(H_2O)_6}$, a comparison with guilleminite, $\mathrm{Ba\,[(UO_2)_3\,(SeO_3)_2\,O_2]\,(H_2O)_3}$. *Can. Mineral.* **39**, 797-807.

Criddle, A.J. & Stanley, C.J., eds. (1993): *The Quantitative Data File for Ore Minerals* (3rd edition). Chapman and Hall, London, U.K.

Dymkov, Yu.M., Loseva, T.I., Zav'yalov, Ye.N., Ryshov, B.I. & Bochek, L.I. (1982): Mgriite, $\mathrm{(Cu,Fe)_3AsSe_3}$, a new mineral. *Zap. Vses. Mineral. Obshchest.* **111**, 215-219 (in Russ.) [also *Int. Geol. Rev.* **25**, 859-863].

________, Ryshov, B.I., Begizov, V.D., Dubakina, L.S., Zav'yalov, Ye.N., Ryab'yeva, V.G. & Tsvetkova, M.V. (1991): Mgriite, Bi-petrovicite and associated selenides from carbonate veins of the Erzgebirge. *In* New Data on Minerals 37. Izdatel'stvo Nauka, Moscow, Russia (81-101; in Russ.).

________, ________, Zav'yalov, Ye.N., Tsvetkova, M.V. & Shcherbachev, D.K. (1989): Bi-variety of petrovicite from dolomitic veins of the Erzgebirge. *Dokl. Akad. Nauk SSSR* **306**, 1451-1455 (in Russ.).

Förster, B. & Haack, U. (1995): U/Pb-Datierungen von Pechblenden und die hydrothermale Entwicklung der U-Lagerstätte Aue-Niederschlema (Erzgebirge). *Z. geol. Wiss.* **23**, 581-588.

Förster, H.-J., Rhede, D. & Tischendorf, G. (2002): Continuous solid-solutions between mercurian giraudite and hakite. *Can. Mineral.* **40**, 1161-1170.

________ & Tischendorf, G. (2001): Se-rich tennantite and constraints on p–T–X conditions of selenide mineral formation in the Schlema–Alberoda uranium ore district (western Erzgebirge, Germany). *Neues Jahrb. Mineral., Abh.* **176**, 109-126.

Harlass, E. & Schützel, H. (1965): Zur paragenetischen Stellung der Uranpechblende in den hydrothermalen Lagerstätten des westlichen Erzgebirges. *Z. angew. Geol.* **11**, 569-582.

Pouchou, J.L. & Pichoir, F. (1985): "PAP" (φ–ρ–Z) procedure for improved quantitative microanalysis. *In* Microbeam Analysis (J.T. Armstrong, ed.). San Francisco Press, San Francisco, California (104-106).

Ryschow, B.I. (1972): Die "Braunspat"-Gänge des Sächsischen Erzgebirges (DDR) und die Stellung der in ihnen befindlichen Selenmineralisation. *Z. angew. Geol.* **18**, 149-157.

Schuppan, W., Büder, W. & Lange, G. (1994): On uranium mineralization in the vein deposits of the western Erzgebirge, Germany. *In* Mineral Deposits of the Erzgebirge/Krušné hory (Germany/Czech Republic) (K. von Gehlen & D.D. Klemm, eds.), Gebrüder Bornträger, Berlin, Germany (191-207).

Shannon, R.D. (1976): Revised effective ionic radii and systematic studies of interatomic distances in halides and chalcogenides. *Acta Crystallogr.* **A32**, 751-767.

Simon, G. & Essene, E.J. (1996): Phase relations among selenides, tellurides, and oxides. I. Thermodynamic properties and calculated equilibria. *Econ. Geol.* **91**, 1183-1208.

________, Kesler, S.E. & Essene, E.J. (1997): Phase relations among selenides, tellurides, and oxides. II. Applications to selenide-bearing ore deposits. *Econ. Geol*. **92**, 468-484.

Stanley, C.J. & Laflamme, J.H.G. (1998): Preparation of specimens for advanced ore-mineral and environmental studies. *In* Modern Approaches to Ore and Environmental Mineralogy (L.J. Cabri & D.J. Vaughan, eds). *Mineral. Assoc. Can., Short Course Ser.* **27**, 111-121.

Sugaki, A., Kitakaze, A. & Odashima, Y. (1981): Furutobeite, a new copper–silver–lead sulfide mineral. *Bull. Minéral.* **104**, 737-741.

Received July 18, 2003, revised manuscript accepted October 30, 2003.